Principles of Selectivity in Fischer-Tropsch SYNTHESIS

Hans Schulz
Engler-Bunte-Institute, University of Karlsruhe
Kaiserstrasse 12, 76128 Karlsruhe, Germany

Abstract

The detailed selectivity of Fischer-Tropsch synthesis with iron and cobalt as catalysts with high temporal resolution has been determined and used to derive the values of probability of chain growth, chain branching and olefin/paraffin molar ratio as a function of carbon number and time. Catalyst reassembling and self-organization of the Fischer-Tropsch regime are investigated. The basic principle of Fischer-Tropsch synthesis, suppression of desorption of growing chains is disclosed. This *frustration* governs FT-synthesis of the otherwise different systems with iron and cobalt. The advanced characterization of sites and elementary reactions (specifically with cobalt) is thought to be a more realistic basis for future theoretical calculations.

Diesel fuel through Fischer–Tropsch synthesis

The present interest in Fischer-Tropsch synthesis focuses on the production of Diesel fuel. Competing in coal liquefaction with hydrogenation [1], the FT-route now is superior because the fuel is very clean and exhibits excellent performance in the combustion engine (**TABLE 1**). However, the maximum selectivity is only ~ 40% C, as shown in **Fig. 1** on the basis of calculating the theoretical product composition, assuming ideal polymerization kinetics with carbon number independent growth probability [2]. The overall Diesel selectivity can be increased to ~ 60% by running the FT-synthesis at high paraffin-wax selectivity (high growth probability pg) and mildly converting the paraffin wax through *ideal hydrocracking*.

TABLE 1 Gas oils from direct coal liquefaction and Fischer-Tropsch synthesis

Gas oil from coal hydrogenation*):

Highly aromatic, Atomic H/C-ratio: 1.3
Phenols: 16 wt-%
Oxygen = 3 wt.-%. Nitrogen = 1.1 wt.%, Sulfur = 0.1 wt.-%
Low cetane rating
Severe hydrogenation/hydrofining necessary:

$$\text{Alkyl-benzenes} + \mathbf{3}\,H_2 \Rightarrow \text{Alkyl-cyclohexanes}$$
$$\text{Alkyl-phenols} + \mathbf{4}\,H_2 \Rightarrow \text{Alkyl-cyclohexanes} + H_2O$$
$$\text{Alkyl-anilines} + \mathbf{4}\,H_2 \Rightarrow \text{Alkyl-cyclohexanes} + NH_3$$
$$\text{Quinoline} + \mathbf{7}\,H_2 \Rightarrow \text{Alkyl-cyclohexane} + NH_3$$

Gas oil from Fischer-Tropsch synthesis:

All aliphatic, atomic H/C-ratio: 2/1
High cetane rating
No sulfur, no nitrogen,
Some oxygen in alcohols, easy to remove
Olefins easy to hydrogenate at low hydrogen consumption
High diesel yield through “ideal hydrocracking” of paraffin wax

*) *W. Krönig, The Bergius process (1977)*

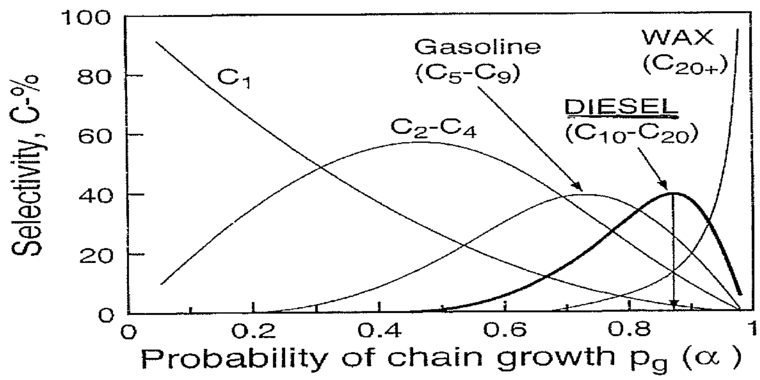

Fig. 1 Product fractions as a function of chain growth probability in Fischer-Tropsch synthesis assuming ideal polymerization kinetics. Adapted from M. Dry (1990)

TABLE 2: Ideal hydrocracking: Primary hydrocracking prevails up to high conversion. The biggest molecules crack preferentially. (H. Schulz et al. 1972)

Feed: n-dodecane, Catalyst: 0.5 Pt on zeolite CaY, Pressure: 40 bar, $n_{H2}/n_{HC} = 20$, LHSV=1 h^{-1}

Reaction temp., °C,	265	275	285	300	
Conversion, %					$\frac{n_{300°C} - n_{285°C}}{n_{285°C}} \times 100$
by cracking	5	17	56	99.5	
by isomerisation	34	48	35	0.47	
	Moles of crack products per 100 moles n-C_{12} cracked				
Methane	-	-	-	0.1	
Ethane	-	-	-	0.1	
Propane	6.7	6.7	7.0	9.0	
Butanes	29.7	30.4	31.8	38.9	
Pentanes	42.3	41.9	41.9	46.3	
Hexanes	43.5	43.5	42.9	44.2	
Heptanes	42.3	41.2	41.0	40.3	- 1.4 %
Octanes	29.5	30.7	30.6	25.9	- 15.0 %
Nonanes	6.3	6.0	5.9	3.4	- 42.0 %
Decanes	-	-	-	-	-
Undecanes	-	-	-	-	-
Sum of moles	200	200	201	208	

The features of ideal hydrocracking are "no" secondary cracking and preference for cracking the biggest molecules in the mixture as demonstrated in **TABLE 2** on the basis of n-dodecane conversion applying the (bifunctional) Pt/Y-zeolite (of particularly high activity for olefin hydrogenation/dehydrogenation and a very high activity/acidity for cracking and isomerization) [3]. The hydroisomerization activity is favorable for high Diesel fuel quality.

Selforganization, reassembling

It has been noticed early: The steady state regime of FT-synthesis is attained during a time (episode) of formation ("Formierung" in the early German literature). The understanding of this process remained poor, however, is of strong technical relevance. Now advanced research tools are available to investigate these phenomena.

Fig. 2 shows how the FT-activity develops as a function of time for an iron- and a cobalt catalyst [4,5,6]. In both cases it needs ~ 4 days until the steady state is attained. With cobalt the Fischer-Tropsch yield increases from ~8% to ~60 % during this time [5]. With iron, initially, the main reaction is carbon deposition [4], (episode I). In episode II the water gas shift reaction - respectively its reverse - develops (under steady carbiding). In episode III - after 2 hours - a first little FT-activity is noticed and only later in episode IV, after about 10 hours, there is a substantial increase of FT-activity, needing about 4 days to establish the steady state. This long duration of activation might indicate that slow processes of solid phase transformation are involved. Inspection of iron catalyst samples from different times of run length with Moessbauer spectroscopy [4] (**Fig. 3**) shows in episode IV - when a first little FT-activity is noticed – the formation of iron carbide (Fe5C2) and the consumption of the metallic iron. *At steady state no metallic iron is present any longer.*

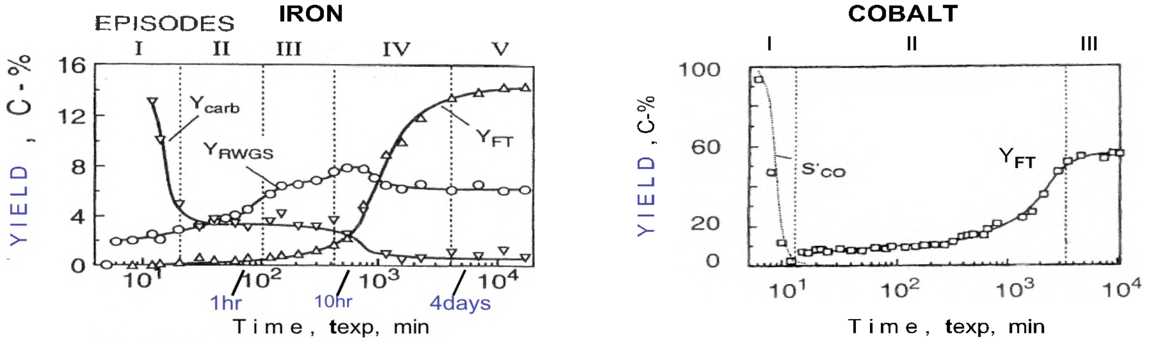

Ref. : Riedel, Schaub, Schulz

Ref. : Thesis Claeys

Yields Y_{FT}: $CO + 2H_2 = (CH_2) + H_2 + H_2O$

Y_{RWGS}: $CO_2 + H_2 = CO + H_2O$

Y_{carb}: $CO = C_{carb} + (O)$

Fig. 2 Selforganization of the Fischer-Tropsch regime, FT-conditions: Iron (Fe-Al-Cu-K) 250°C, 10 bar, H2/CO=3:1, Cobalt (Co-Zr-Pt-Aerosil); 190°C, 5 bar, H2/CO=2:1 [3, 4, 5]

IRON

COBALT

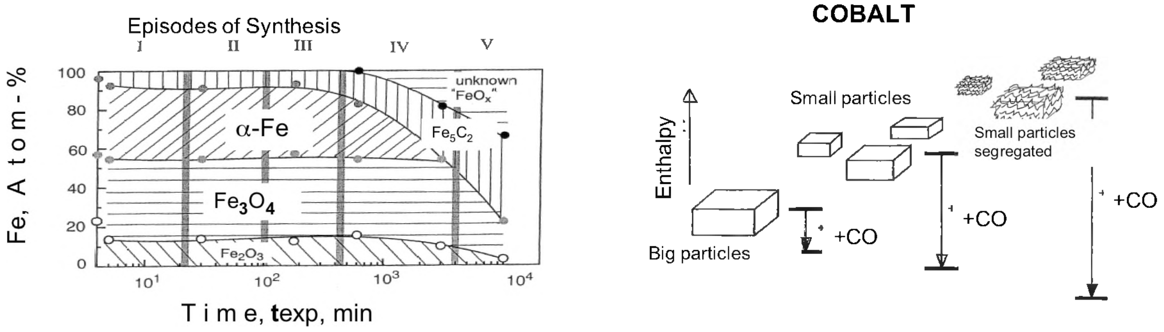

Iron phase composition
by Moessbauer spectroscopy

Catalyst: 100Fe-13Al-11Cu-9K

FT-Synthesis: 250°C,10 bar, $H_2/CO_2 = 3:1$

Thermodynamic view of ***cobalt surface segregation*** in FT-synthesis

Sites disproportionation for low and high coordination (on-top and hollow)

Fig. 3 Catalyst selfassembling [4,6,7]

The XRD-spectra of catalyst samples [4] (**Fig. 4**) confirm the result that at steady state no metallic iron is present. In consequence, with iron catalysts, the true FT-catalyst is not the metallic iron. It must be attributed to a different iron phase, most probably to the (alkalized) iron carbide phase - in collaboration with the (alkalized) oxidic iron phases which are also active for the water gas shift reaction, this includes activation of hydrogen

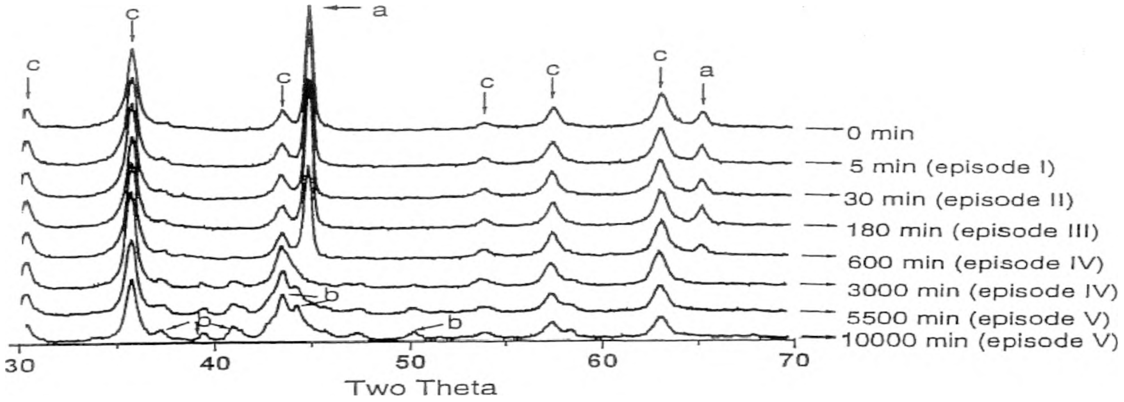

a Metallic iron **b** Iron carbide (Fe_5C_2) **c** Magnetide (Fe_3O_4)

FT-Synthesis: Catalyst: 100Fe-13Al-11Cu-9K; 250°c, 10 bar, $H_2/CO_2 = 3:1$

Fig. 4 XRD Spectra of iron catalyst samples from different FT-run lengths [4]

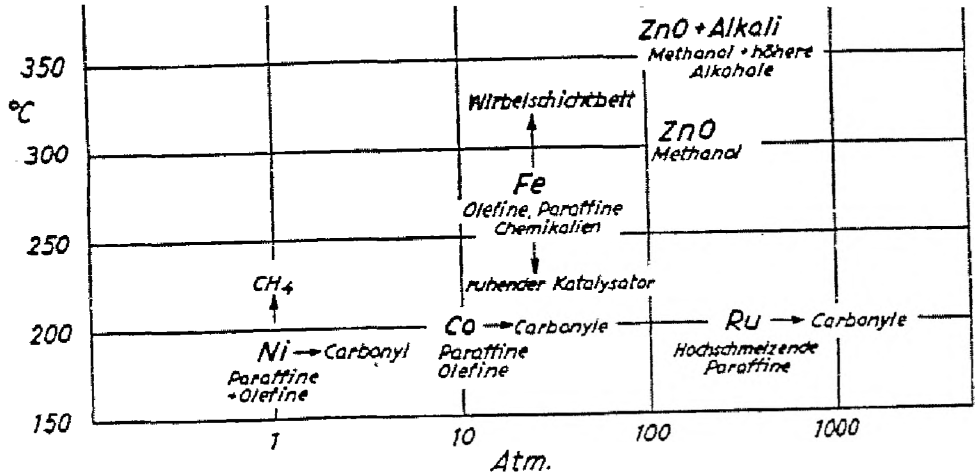

Fig.5 Temperature/pressure ranges of catalysts in CO-hydrogenation (H. Pichler 1952)

With cobalt as the catalyst, it appears that activation follows a different route (**Fig. 3,right**) [6, 7]. Through strong CO-chemisorption the surface of cobalt crystallites is roughened [8] and thereby enlarged for more CO to be adsorbed. This surface segregation involves sites disproportionation for low and high coordination and the two sorts of sites are suggested to cooperate for chain growth on the on-top sites and CO-dissociation and CH2-monomer formation on the hollow sites [6,7]. Regular cobalt crystallite surface plains segregation through Fischer-Tropsch synthesis has been observed by means of scanning tunneling electron microscopy [8]. Support for this view on catalyst restructuing comes from former work in FT-synthesis, reviewed by Pichler [9] pointing out that FT-synthesis on cobalt (nickel and ruthenium) performs at pressures just below of carbonyl formation from the catalytic metals. Pichler therefore suspected "surface carbonyl complexes" as the true FT-catalysts (**Fig. 5**). This is in line with a *continuous transition from heterogeneous to homogeneous catalysis* - from Fischer-Tropsch synthesis to hydroformylation.

Chain growth

In ideal polymerization the probability of chain prolongation would be independent of chain length, representing a horizontal line in the diagram of prolongation probability as a function of carbon number.

The values of growth probability are calculated from experimental values of product composition [10,11]. **Fig. 6** shows such curves for FT-synthesis on iron and cobalt at different times during self-organization of the FT-regime [4,12].

With iron the curves are not so far from horizontal lines, as relating to ideal polymerization behavior. The value at Nc=1 is not lower than the values at higher carbon numbers, meaning no preferred methanation. During catalyst reassembling the

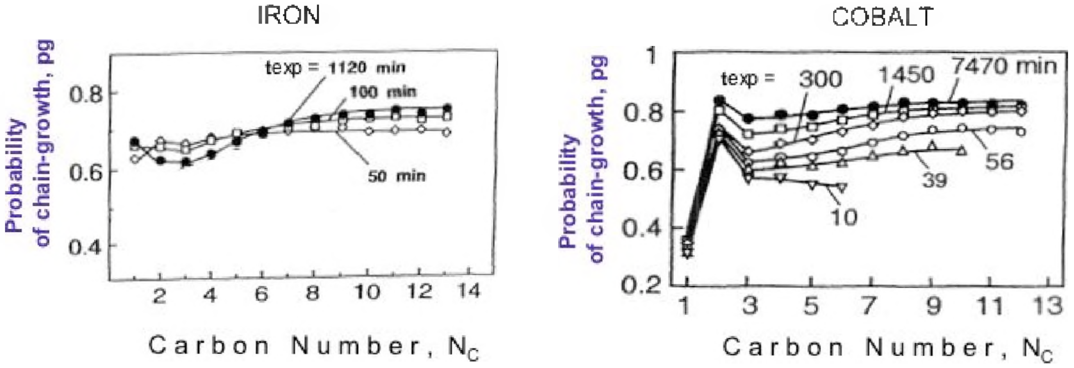

Fig. 6 Chain prolongation probability pg as a function of carbon number Nc for different run length with iron and cobalt as the catalysts [4,12]

FT-synthesis: **Iron** (100 Fe-13Al-11Cu-25K); 250°C, 10 bar, H2/CO=2.3/1. **Cobalt** (97 Co-12Zr-100Aerosil); 190°C, 5 bar, H2/CO=2/1

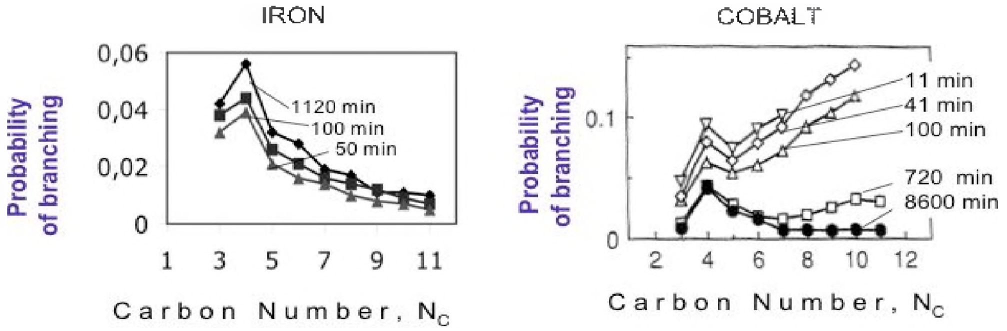

Fig. 7 Chain branching
FT-synthesis: **Iron** (100 Fe-13Al-11Cu-25K); 250°C, 10 bar, H2/CO=2.3:1. **Cobalt** (97 Co-12Zr-100Aerosil); 190°C, 5 bar, H2/CO=2/1 [4,12]

curves vary not so much. Evidently, the surface chemistry of FT-catalysis on iron is not changing, in spite of the drastic changes of catalyst composition and structure: The kind of FT-sites remains just the same from the beginning.

With cobalt (**Fig. 6 right**) the pg-value at Nc=1 is very low, referring to a pronounced methanation (as thermodynamically preferred, however, suppressed in the FT-regime). In contrast to iron, the average value of growth probability increases from ~0. 6 to ~0.8 (see range C3 to C10 in the figure). This indicates the polymerization nature to develop with time, as the true catalyst is being "constructed.

Typically, the chain growth proceeds linearly, however, also compounds with methyl side groups are noticed, as referring to a distinct probability of branching pbr (**Fig. 7**), [4,7,12].

The observed trends are the following: 1) The first value of pbr at Nc=3 is low, reflecting a suppressed desorption probability after a branching step (caused by spatial constraints arising from methyl branching at the adjacent C-atom). 2) From Nc=4 to higher carbon numbers the branching probability decreases strongly. This is attributed to increasing spatial constraints with increasing size of the chain.

3) With cobalt and iron, the trends with increasing time on stream are opposite, relating to differences in catalyst reassembling. With iron the spatial constraints decrease, with cobalt they increase. 4) Initially with cobalt, the branching probability is comparatively high and shows a different pattern of chain length dependence (**Fig 7, right**): an *increase* with carbon number(from Nc=5 to Nc=10). This indcates a different additional mechanism: the adsorption of olefins with their β-C-atom (whereas at steady state FT conditions the spatial constraints are stronger and allow only re-adsorption of olefins with their terminal C-atom.

Olefin selectivity

The olefin contents in carbon number fractions are shown in **Fig. 8**. The curves pattern is different for FT on iron- and cobalt catalysts. With cobalt it reflects secondary olefin hydrogenation [7,13]. This is extensive at C2 because of a high ethene reactivity. It increases from C3 to higher olefins, due to increased adsorption probability. During cobalt surface restructuring, secondary olefin hydrogenation is increasingly suppressed. With iron there are almost no signs of secondary olefin hydrogenation in the product composition, the value at C2 merely differs from those at higher carbon number. Here, the olefin/paraffin molar ratio reflects relative desorption probabilities of the chains from the growth sites - as olefin or as paraffin. At steady state the desorption as olefin is favored against the desorption as paraffin (70 – 80 %).

Secondary olefin hydrogenation is associated with secondary **olefin isomerization**. It is seen in **Fig. 9** that on iron the olefins are to more than 90 % olefins with their double bond in terminal position, referring to (almost) no secondary double bond shift in the system, neither at the steady state nor during self-organization. With cobalt, fast double bond shift accompanies secondary hydrogenation, and the olefins are only to a minor part to those with terminal double bonds. **Fig. 10** refers to the kinetic schemes of olefin formation and secondary reactions .

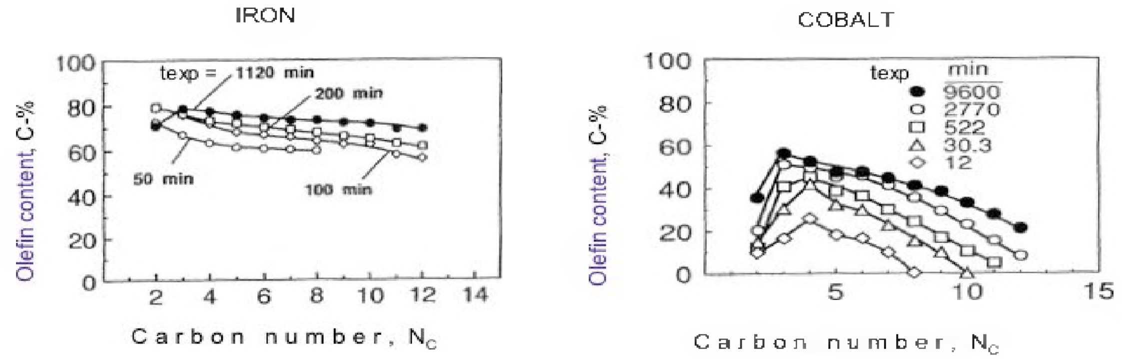

Fig. 8 Olefin content in carbon number fractions (further legend as in Fig. 9)

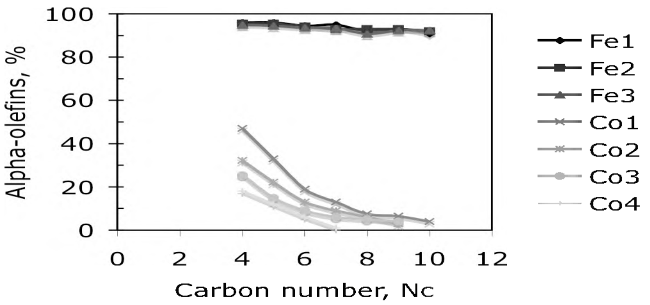

Fig. 9 Olefin-1 contents in olefin carbon number fractions at different times t_{exp}.Upper curves **Iron** (100 Fe-13Al-11Cu-25K); 250°C, 10 bar, H2/CO=2.3:1.Lower curves **Cobalt** (97 Co-12Zr-100Aerosil); 190°C, 5 bar, H2/CO=2/1

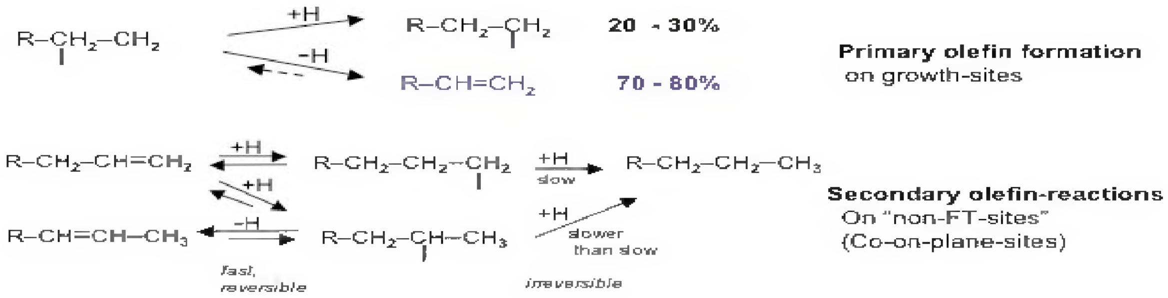

Fig .10 Kinetic schemes of olefin reactions

Structure sensitivity

In heterogeneous catalysis, the concept of relating catalyst activity to the number of active sites (turn over number) is frequently used. However, in FT catalysis it appears to be not applicable (**Table 3**).

The common FT principle for iron and cobalt catalysts.

Iron and cobalt as FT catalysts are compared in **Table 4**. Several principal differences are noticed. The common mechanistic feature is suggested as "frustration" of alkyl-desorption (. This allows chain growth with the available monomers (CH2, CO, C2H4).

Selectivity for FT sites characterization

The ordered complexity of product composition with many more than 100 compounds reflects the nature of the active sites in detail. From the various possible reactions just a distinct set is chosen, others (even those thermodynamically favored) being frustrated. Conclusions rely on the precision of product analyses and mass balances this with high temporal resolution (methods of quick product sampling and wide range, high resolution gas chromatography together with the right reaction engineering have been developed [14]. **Figs. 11, 12** show chromatograms from FT ampoule samples (sampling duration is less than 0,1 second) with and without pre-column hydrogenation. Small peaks of compounds with a selectivity of e.g. 0.5C-% are still determined with a GC-common accuracy of about 1-5% of the value. The chromatogram range covers the compound carbon numbers C1 to C20. A high potential for quantitative evaluation is evident.

TABLE 3 Turnover concept in Fischer-Tropsch synthesis ???

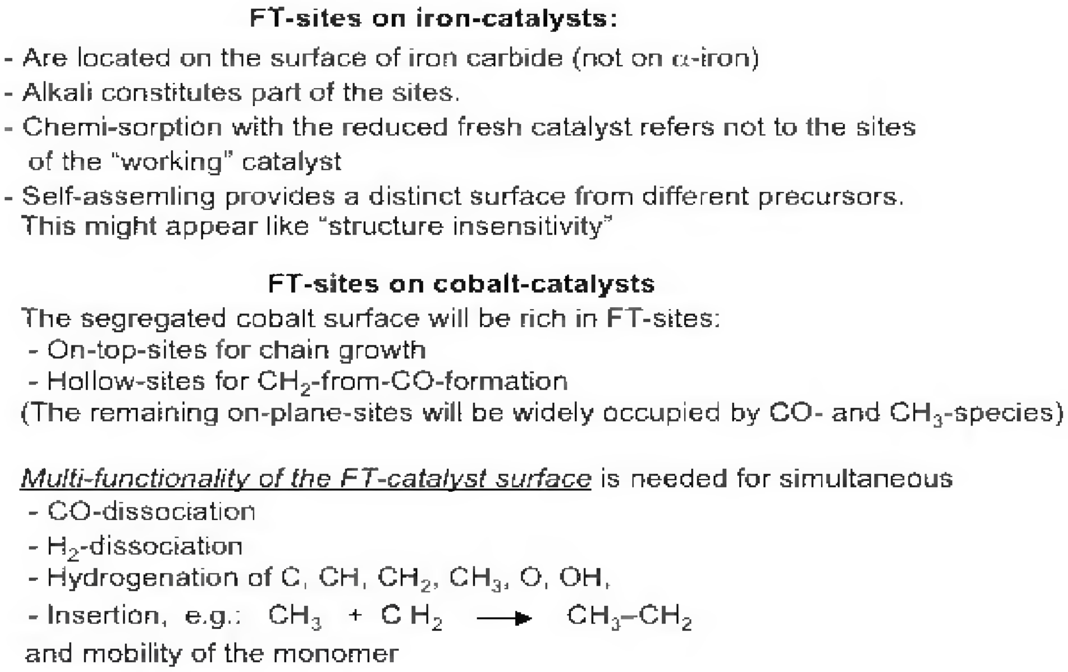

FT-sites on iron-catalysts:

- Are located on the surface of iron carbide (not on α-iron)
- Alkali constitutes part of the sites.
- Chemi-sorption with the reduced fresh catalyst refers not to the sites of the "working" catalyst
- Self-assemling provides a distinct surface from different precursors. This might appear like "structure insensitivity"

FT-sites on cobalt-catalysts

The segregated cobalt surface will be rich in FT-sites:

- On-top-sites for chain growth
- Hollow-sites for CH_2-from-CO-formation

(The remaining on-plane-sites will be widely occupied by CO- and CH_3-species)

Multi-functionality of the FT-catalyst surface is needed for simultaneous

- CO-dissociation
- H_2-dissociation
- Hydrogenation of C, CH, CH_2, CH_3, O, OH,
- Insertion, e.g.: $CH_3 + CH_2 \longrightarrow CH_3{-}CH_2$

and mobility of the monomer

TABLE 4 Comparing iron and cobalt as catalysts for FT-synthesis

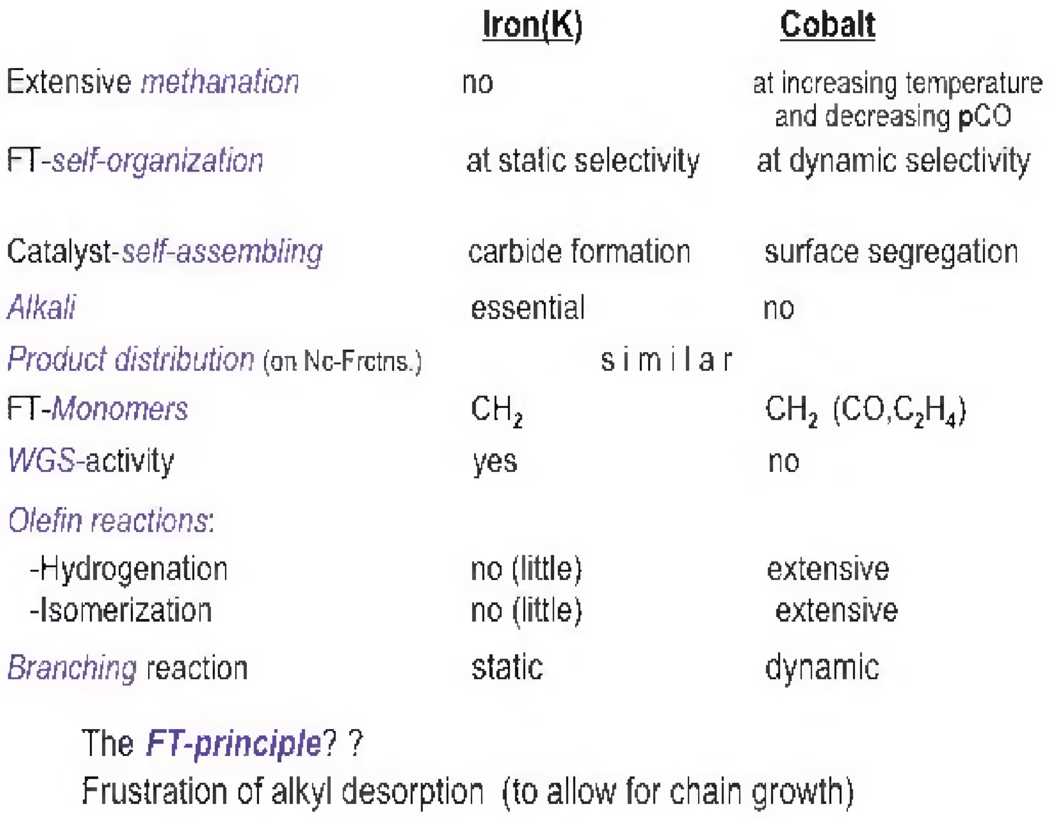

	Iron(K)	Cobalt
Extensive *methanation*	no	at increasing temperature and decreasing pCO
FT-*self-organization*	at static selectivity	at dynamic selectivity
Catalyst-*self-assembling*	carbide formation	surface segregation
Alkali	essential	no
Product distribution (on Nc-Frctns.)	similar	
FT-*Monomers*	CH_2	CH_2 (CO, C_2H_4)
WGS-activity	yes	no
Olefin reactions:		
-Hydrogenation	no (little)	extensive
-Isomerization	no (little)	extensive
Branching reaction	static	dynamic

The ***FT-principle***? ?

Frustration of alkyl desorption (to allow for chain growth)

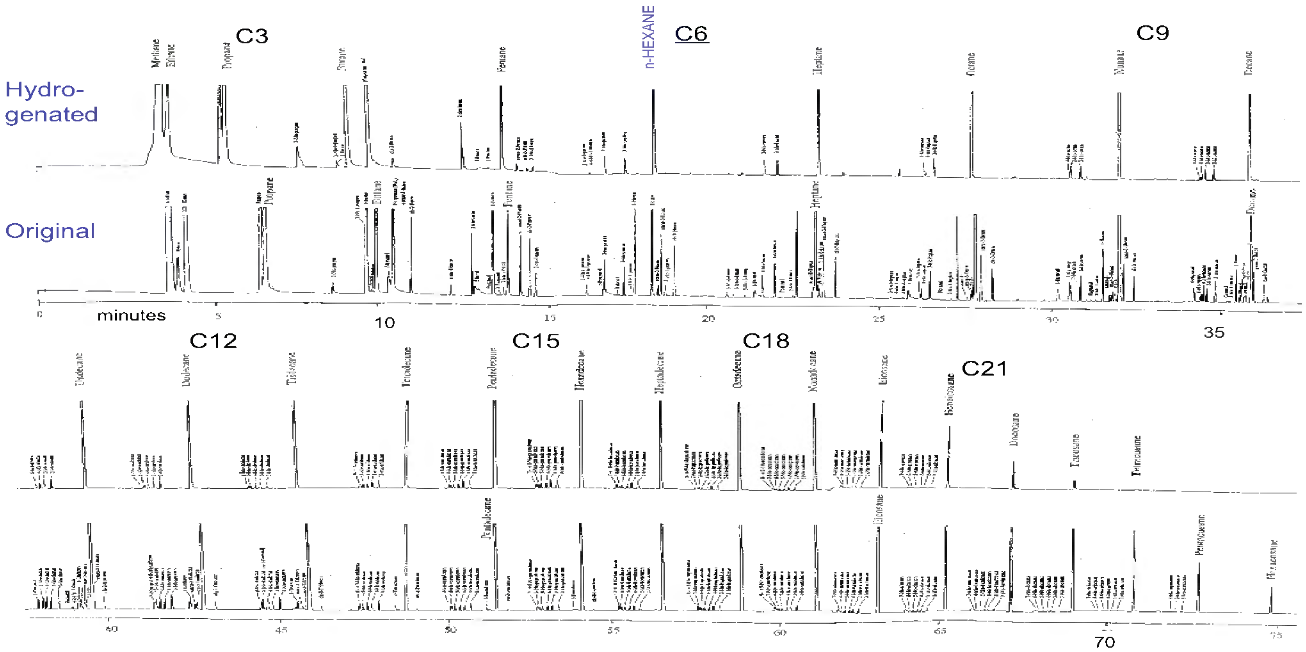

Fig. 11 Chromatograms of FT product ampoule samples (original and hydrogenated)

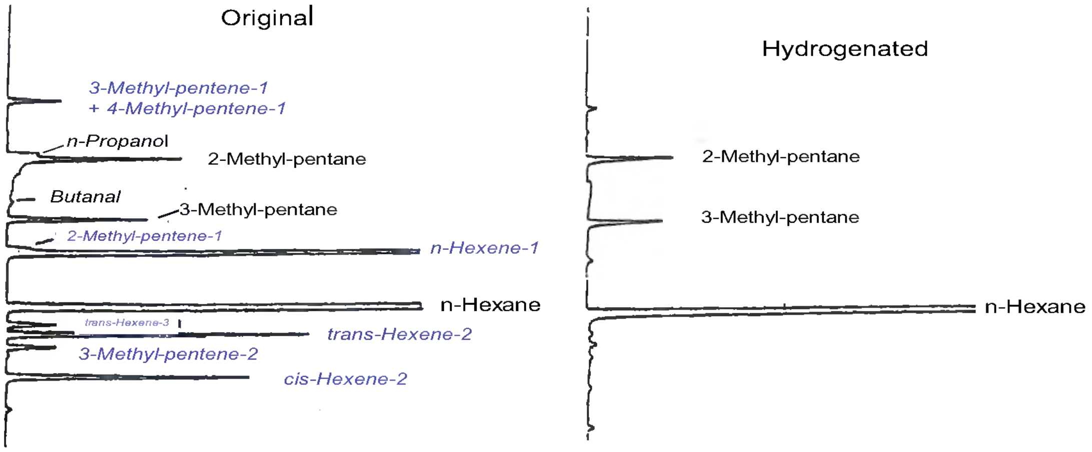

Fig. 12 C6-fraction enlarged from Fig. 11

Literature

1. W. Krönig, "*Kohlehydrierung*" in Chemierohstoffe aus Kohle ,J. Falbe (Ed.), Georg Thieme Verlag, Stuttgart (1977) 272
2. M. Dry, Catalysis Today 71 (2002) 227
3. H. Schulz, J. Weitkamp, Ind. Eng. Chem., Prod. Res. Develop. 11 (1972) 46
4. T. Riedel, H. Schulz, G. Schaub, K.-W. Jun, J.-S. Hwang, K.-W. Lee, Topics in Catalysis 26 (2003) 41
5. M. Claeys, Ph.D.-Thesis, Karlsruhe (1997)
6. H. Schulz, Zh. Nie, F. Ousmanov, Catalysis Today 71 (2002) 351
7. H. Schulz, Topics in Catalysis 26 (2003) 73
8. J. H. Wilson, C.M.P. de Groot, J. Phys. Chem. 99 (1995) 7860
9. H. Pichler, Advances in Catalysis, 4 (1952) 271
10. H. Schulz, M. Claeys, Appl. Cat. A: General 186 (1999) 91
11. H. Schulz, K. Beck, E. Erich, Stud. Surf. Sci. Cat. 36 (1988) 475
12. Zh. Nie, Ph.D.-Thesis, Karlsruhe (1996)
13. H. Schulz, M. Claeys, Appl. Cat. A: General 186 (1999) 71